

STRUCTURAL AND OPTICAL PROPERTIES OF RARE EARTH DOPED PHOSPHATE GLASS CONTAINING NANOPARTICLES

M. R. Sahar*, E. S. Sazali, Raja J. Amjad

Advanced Optical Material Research Group, Department of Physics, Faculty of Science,
Universiti Teknologi Malaysia, 81310, Skudai, Johor Bahru, Johor, Malaysia.

*E-mail: mrahim057@gmail.com

Abstract

Transparent rare earth doped phosphate based glasses with and without silver nanoparticles (NPs) are obtained using conventional melt-quenching technique. In the present study, structural properties of glass are investigated by using X-ray Diffraction (XRD) and Transmission Electron Microscopy (TEM). In addition, the optical properties of glass are investigated by means of UV-Vis-NIR and Photoluminescence (PL). The amorphous nature of the glass is confirmed by XRD diffractogram. TEM studies revealed the nano-crystals glass morphology which is associated to the existence of crystallized phase. It is found that the growth of particle size of silver in glass matrix depends mainly on the diffusion coefficient and activation energy of coalescence and more specifically on the heat treatment time and temperature of the matrix. For UV-Vis-NIR studies, the absorption spectra of RE doped phosphate with NPs presents several sharp absorption bands due to the respective transitions of RE ions which has been transit from the ground state to the excited states. With the addition of NPs, the wavelengths of the absorption peaks are almost unchanged but the cut-off absorption bands shift to shorter wavelengths. The emission peaks for the luminescence were found to be located at the wavelength which corresponding to each rare earth. The enhancement of RE luminescence is due to the presence of NPs. The large luminescence enhancement was obtained due to the simultaneous contribution of the RE energy transfer. Our findings may provide some useful information towards the development of functional glasses with controlled optical properties.

Keywords: Rare earth (RE), Nanoparticles (NPs)

1. Introduction

Interest in materials containing rare-earth (RE) ions and metallic nanoparticles (NPs) including gold and silver are expected for the intensification of luminescence [1, 2]. Metallic nanoparticles exhibit unique optical response and enhanced electromagnetic field and constitute the area of "plasmonics" [2]. Rare-earth doped glasses containing metallic NPs are attractive because the presence of NPs can enhance the UC luminescence due to the potential application to full color display, laser antiforgery and bio-label to cite a few and the non-linear properties suitable for device applications [2 - 4]. Among the materials of current interest, phosphate glass containing rare earth element are expected for applications in optical data transmission, detection and laser technologies [5]. Phosphate glasses are very good candidates for these studies because they have high transparency, low melting point, high thermal stability, high gain density, high solubility for rare-earth ions, low refractive index and low dispersion [6]. Moreover, the assimilation of RE³⁺ can stabilize the metastable crystalline phase which leads to a development of optical devices based [7, 8]. The RE doping into nano-crystalline glass has great implications over the properties of glass which expected for use in nonlinear optical devices because of their large

third-order nonlinear optical susceptibility [9]. Recently, the fabrication nucleation of metallic NPs in selenite tellurium oxide glasses have been reported [1, 10, 11]. The focus in this work is to examine the effect of silver NPs in Er³⁺ doped phosphate glass. The structural studies are verified using XRD and TEM. The optical properties are confirmed using UV-Vis-NIR and Photoluminescence.

2. Experimental

Series of glass based on P₂O₅- MgO - AgCl doped with constant Er₂O₃ concentration and in addition of silver NPs are prepared by using the melt quenching technique. XRD measurement is performed on Siemens Diffractometer D5000. Diffraction patterns were collected in the 2θ range from 15° to 75°, in steps of 0.05° and 1s counting time per step and using Cu Kα as a radiation source of wavelength λ=1.54056Å. A 200kV TEM 2100, JEOL is used to investigate the nucleation of silver NPs embedded in the glass matrix. Optical absorption spectra are measured at room temperature in the 400-1700 nm range using a Shimadzu 3101 UV-Vis-NIR. The absorbance signal is analyzed using a double monochromatic diffraction grating system and photomultiplier R-928 detector with resolution is about 0.1nm. To

determine the excitation and emission throughout all samples, the Photoluminescence measurement is conducted on Nanosecond Luminescence Spectroscopy System, Ekspla Model NT340/1 tunabled Nd: YAG laser system. Each sample in powder form is placed in the spectrometer and scanned for radiation spectral wavenumber in the range of $200 - 900 \text{ cm}^{-1}$ at room temperature. The Xenon lamp ($300 < \lambda < 1300\text{nm}$) was used as a pumping source.

3. Results and Discussion

Figure 1 shows the result of X-ray Diffraction (XRD) pattern for phosphate glass as function of 2θ scale. It can be seen that there are no sharp peaks presents in spectra. The halo pattern indicates the characteristic of the amorphous state.

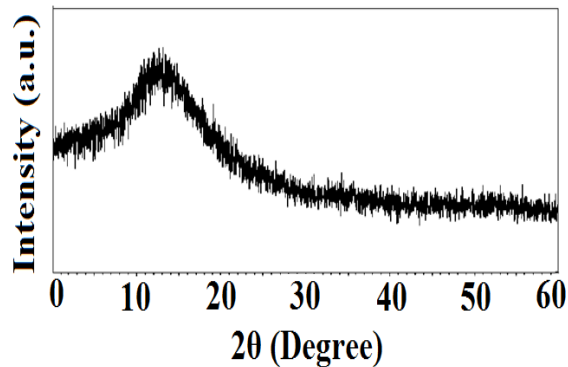


Figure 1: X-ray diffraction patterns for the 59.5 P₂O₅-40 MgO-0 AgCl-0.5 Er₂O₃glass system.

The existence of crystalline phase is then verified by TEM analysis. TEM micrographs show the general crystal morphologies of the resultant microstructures after crystallization as taken in the secondary electron imaging (SEI) mode. Figure 2 shows the TEM micrographs of 58 P₂O₅-40 MgO-1.5 AgCl-0.5 Er₂O₃glass systems which clearly displays an overall spherical shape of silver NPs. Inset shows the selected area electron diffraction (SAED) of the glass system. Bright spots in the SAED pattern indicate the presence of silver NPs. Fig. 2 (b) shows the high-resolution TEM image of a single NP formed in the glass system. The NPs formed in this glass have cubic close packed structure which is evidence by the fast Fourier transformation of image 2 (b). The obtained lattice constant is 2.13\AA which is comparable to that of bulk Ag ($d_{200} = 2.05\text{\AA}$, JCPDS No. 030931). Therefore, the NPs observed in the glass are the silver NPs indeed. Fig. 2 (c) shows the corresponding histogram of the sizes distribution of silver NPs with average diameter of 37 nm.

Figure 3 shows the absorbance spectra of ofEr³⁺ doped phosphate glass without silver NPs and with varying concentration of silver NPs such as 0.5mol%, 1.0 mol% and 1.5 mol% silver NPs.

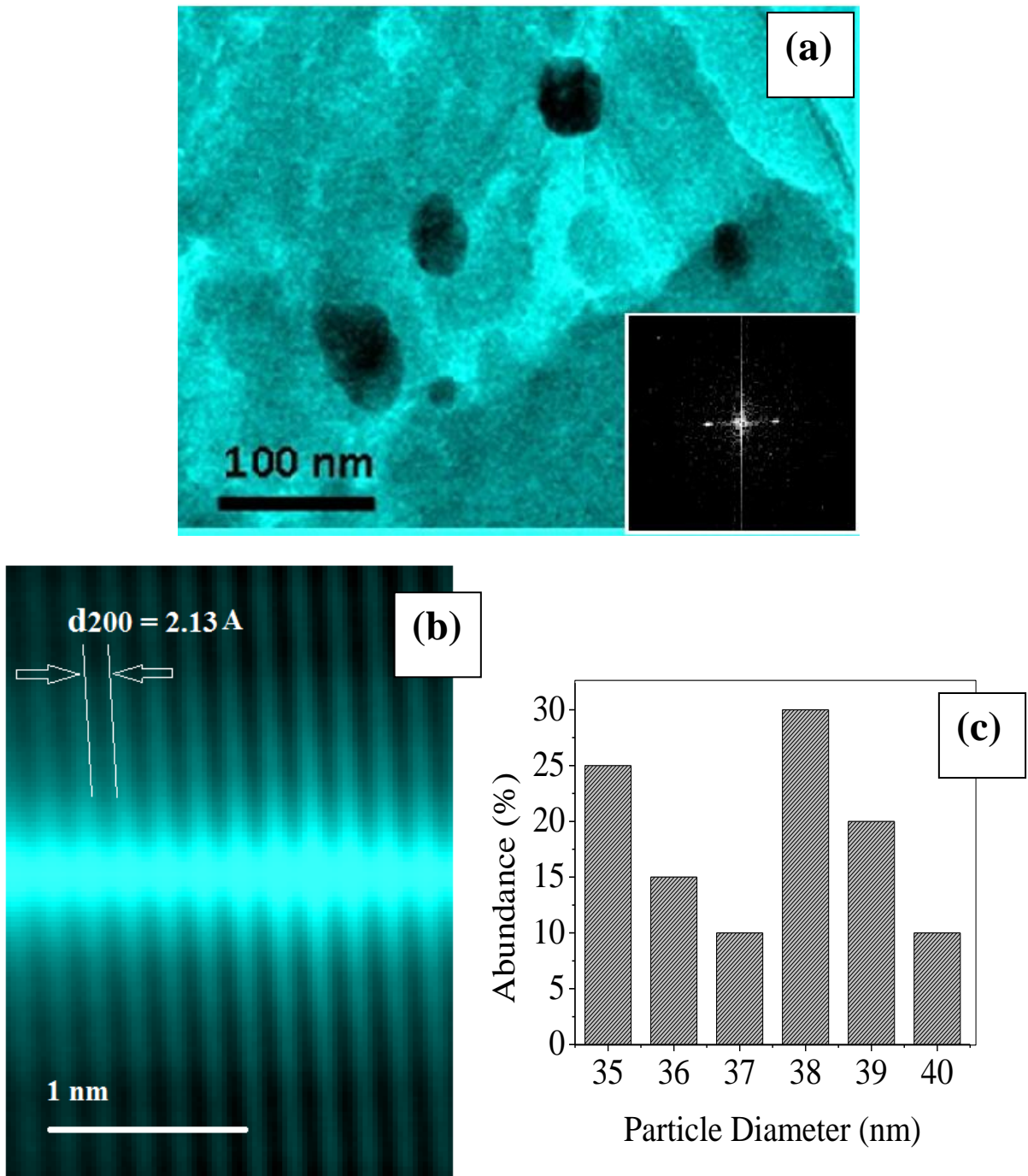


Figure 2. (a) TEM image of 58 P_2O_5 -40 MgO -1.5 $AgCl$ -0.5 Er_2O_3 glass system. Inset shows selected area electron diffraction pattern (SAED) of the glass D; (b) High-resolution TEM image of one single NP; (c) Histogram of the size distribution of the metallic NPs. Average diameter: 37 nm.

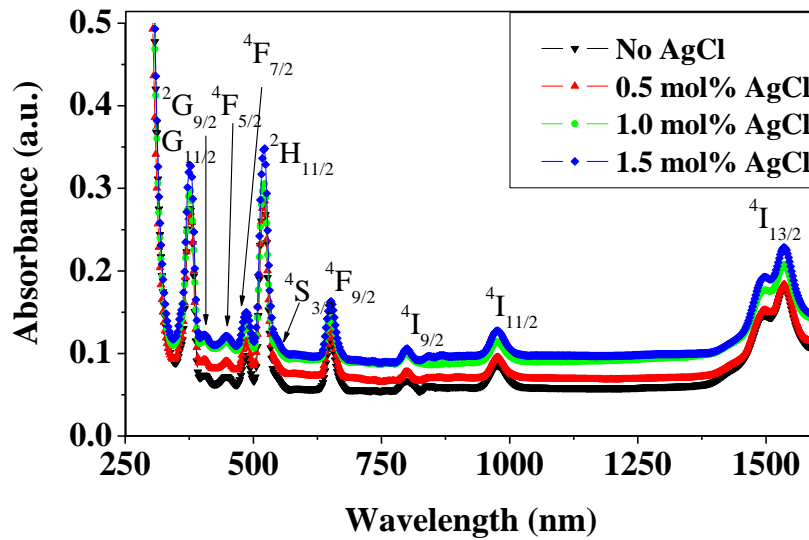


Figure 3. Absorption spectra of Er^{3+} doped phosphate glass (a) without silver NP, (b) with 0.5 mol% AgCl, (c) with 1.0 mol% AgCl and (d) with 1.5 mol% AgCl

Five excited levels corresponding to ${}^4I_{13/2}$, ${}^4I_{11/2}$, ${}^4I_{9/2}$, ${}^4F_{9/2}$, ${}^4S_{3/2}$, ${}^2H_{11/2}$, ${}^4F_{7/2}$, ${}^4F_{5/2}$, ${}^2G_{9/2}$, ${}^4G_{11/2}$ are observed. The assignments of overlapped ${}^{2s+1}L_J$ levels are difficult and are shown in Fig.4. It is evident that the most intense transitions are ${}^2H_{11/2}$ and ${}^4G_{11/2}$ and there is even more enhancement in

the presence of silver NPs which is clearly indicated by Fig.4 in the variation of peak absorbance as a function of AgCl concentration. Addition of silver enhances the corresponding absorption and is maximum for 1.5 mol% AgCl which is evident from Fig.3. This enhancement in absorbance was due to the principal role played by the silver NPs.

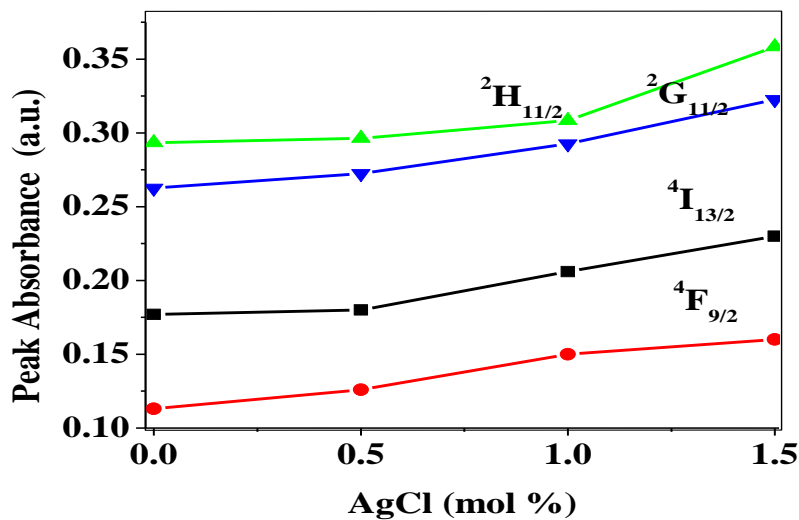


Figure 4. Peak absorbance versus AgCl concentration for different transitions.

For the UC spectra the excitation wavelength was 797nm. Fig.5 shows the UC spectra for Er^{3+} doped phosphate glass without silver NPs and with silver NPs of varying concentration of 0.5mol%, 1 mol% and 1.5 mol%. Two UC bands located at 540nm and 632nm are observed in all titled glasses and are assigned to arise due to $^4\text{S}_{3/2} - ^4\text{I}_{15/2}$ and $^4\text{F}_{9/2} - ^4\text{I}_{15/2}$ transitions respectively. From Fig.5 it is clear that the UC intensity enhanced with increasing the NPs concentration. It is important to note that the relative intensity increment in the green band is higher compared to red one (see Fig.6). The excitation mechanism is shown schematically in energy level diagram of the Er^{3+} ion (Fig.2).

The first incident photon is absorbed by the Er^{3+} ion and it is promoted to the higher energy level $^4\text{I}_{9/2}$ ($^4\text{I}_{15/2} \rightarrow ^4\text{I}_{9/2}$). The excited ions in the $^4\text{I}_{9/2}$ state decay non-radiatively to the lower excited state $^4\text{I}_{11/2}$. From the excited state $^4\text{I}_{11/2}$, Er^{3+} ions absorb another photon and promoted to $^4\text{F}_{5/2}$, $^4\text{F}_{3/2}$. The excited ions in the $^4\text{F}_{3/2}$, $^4\text{F}_{5/2}$ levels decay non-radiatively to the lower excited states $^4\text{F}_{7/2}$, $^2\text{H}_{11/2}$ and $^4\text{S}_{3/2}$. The Er^{3+} ions from $^4\text{S}_{3/2}$ decay radiatively to ground state via $^4\text{S}_{3/2} \rightarrow ^4\text{I}_{15/2}$ and non-radiatively to $^4\text{F}_{9/2}$ state followed by radiative decay

via $^4\text{F}_{9/2} \rightarrow ^4\text{I}_{15/2}$ transition. As stated earlier there is an enhancement in the UC emission intensity in the presence of silver NPs and as the concentration of silver NPs increases the UC emission intensity also increases. This enhancement can occur due to the local field effect of silver NPs or by transfer of energy from silver plasmon bands to Er^{3+} ions.

The emergence of plasmon band seems less likely since the plasmon band of silver NPs is far away from the excitation wavelength 797nm. Therefore, the UC intensity enhancement is due to the local field effect of the silver NPs resulting from the mismatch between the dielectric functions of the glass and silver NPs.

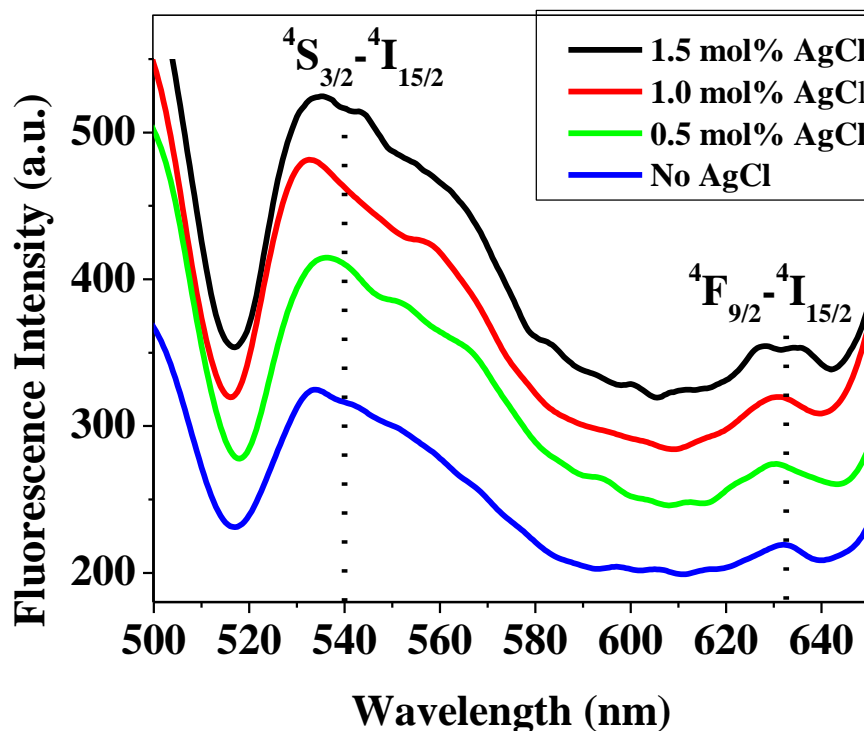


Figure 5. Upconversion spectra for excitation at 797nm.

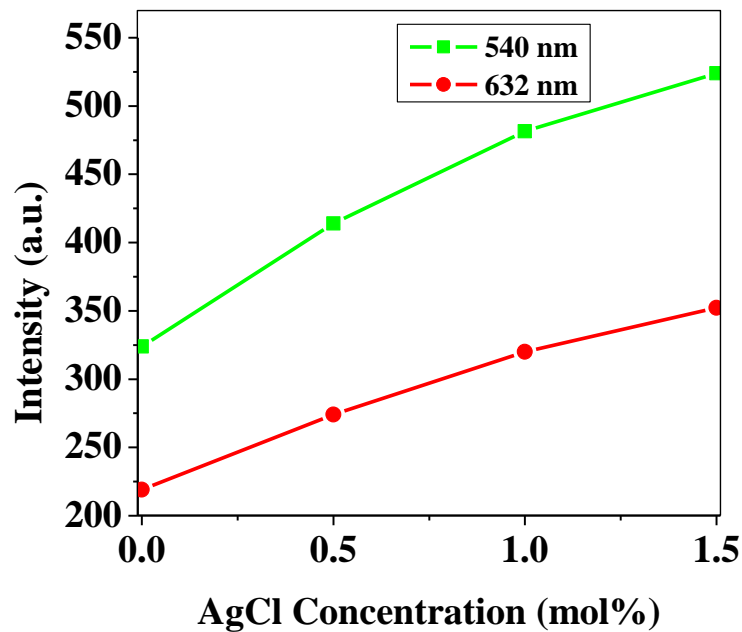


Figure 6. Effect of AgCl Concentration On the fluorescence bands due to Er^{3+} ion

4. Conclusion

Series of glass system based on P_2O_5 - MgO – AgCl doped with constant Er_2O_3 and an addition of silver NPs have successfully been obtained using conventional melt quenching technique. The glass shows good quality as they are visually transparent. The halo pattern of XRD spectra confirms the amorphosity of as-cast glass. TEM study reveals the presence of silver NPs of almost spherical shape and various in sizes laid down in the glass matrix depending on the AgCl concentration. Addition of silver NPs enhances the corresponding absorption and the maximum enhancement is found for 1.5 mol% AgCl. The influence of silver NPs in enhancing the luminescence properties is described.

Acknowledgments

The authors gratefully acknowledge the financial support from Ministry of Higher Education through grant Vot. 4F083 and Universiti Teknologi Malaysia under Vot. 02J77 (GUP/MOHE).

References

- [1]. Ricardo de Almeida, Davinson, M. Da Silva, Luciana, R. P., Kassab and Cid B. de Araujo (2008). Eu^{3+} Luminescence in Tellurite Glasses with Gold Nanostructures. *Optics Communications*. **281**, 108–112.
- [2]. Prasad, P. N. (2004). *Nanophotonics*, Wiley-Interscience, New York.
- [3]. Digonnet, M. J. (1993). *Rare Earth Doped Fiber Lasers and Amplifiers*, Dekker, New York.
- [4]. Hamanka, Y., Nakamura, A., Omi, S., Del Fatti, N., Vallee, F., Flytzanis, C. (1999). Ultrafast response of nonlinear refractive index of silver nanocrystals embedded in glass, *J. Appl. Phys. Lett.* **75** 1712-1715.
- [5]. Hayakawa, T., Selvan, S., Nogami, M. (1999). Field enhancement effect of small Ag particles on the fluorescence from Eu^{3+} -doped SiO glass, *J. Appl. Phys. Lett.* **74**, 1513-1515.
- [6]. Suratwala, T. I., Steele, R. A., Wilke, G. D., Campbell, J. H., and Takeuchi, H. (2000). Effects of OH content, water vapor pressure, and temperature on sub-critical crack growth in phosphate glass, *J. Non-Cryst. Solids* **263-264**, 213-227.
- [7]. Wang, J. S., Vogel, E. M., Snitzer, E. (1994). 1.3μ emission of neodymium and praseodymium in tellurite-based glasses. *J. Non-Cryst. Solids*. **178**, 109-113.
- [8]. Luciana, R. P., Kassab, Ricardo de Almeida, Davinson M. da Silva, Thiago A. A. De Assumpcao, and Cid B. D Araujo (2009). Enhanced Luminescence of Tb^{3+}/Eu^{3+} Doped Tellurium Oxide Glass Containing Silver Nanostructures. *J. Appl. Phys.* **105**, 103505.
- [9]. Wang, J. S., Vogel, E.M. and Snitzer, E. (1994). 1.3μ Emission of Neodymium and Praseodymium in Tellurite-Based Glasses, *J. Non-Cryst. Solids*, **178** 109-113.
- [10]. Rai, V. K., Menezes, S., C. B. de Araujo, Kassab, L. R. P., D. M. daSilva, and R. A. Kobayashi (2008). *J. Appl. Phys.* **103**, 093526.
- [11]. C. B. de Araujo, L. R. P. Kassab, R. A. Kobayashi, L. P. Naranjo, and P. A. S. Cruz (2006). *J. Appl. Phys.* **99**, 123522.